Nonsingular Terminal Sliding-mode Lateral Control of an Autonomous Vehicle with Global Fixed-time Stability Guarantees

Moussa Labbadi, Olivier Sename

Nonsingular Terminal Sliding-mode Lateral Control of an Autonomous Vehicle with Global Fixed-time Stability Guarantees

Moussa Labbadi[1] and Olivier Sename[1]

***Abstract*— The present paper develops an output feedback fixed-time sliding mode control (FxTSMC) approach for lateral trajectory tracking of an autonomous vehicle subject to disturbances. Firstly, a nonsingular terminal sliding manifold is constructed to force the orientation error and lateral deviation to converge to desired values in finite time. Secondly, using variable exponent coefficients, a switching control law is proposed to provide fixed-time stability against external disturbances. By adjusting the control design parameters, the upper bound of the settling time for the closed-loop lateral system can be attained arbitrarily minimal without depending on the systems initial conditions. The effectiveness of FxTSMC is demonstrated by comparing the performance of closed-loop systems of the supplied controller and other existing controllers.**

***Index Terms*— Sliding mode control, Fixed-time stability, Autonomous vehicle, Lateral control, Automotive control.**

I. Introduction

Lateral control of autonomous vehicles mainly consists in following a predefined trajectory, given by a path planning algorithm. By adjusting the steering actuator, the lateral error is minimized, and the lane-keeping/lane-changing objectives are achieved. Many papers have investigated and focused on the lateral dynamics, see the survey papers [1], [2].

Different control approaches have been applied to the lateral control problem. In [3], a comparative study of Linear Parameter Varying controllers was presented. The authors of [4] developed a fuzzy controller for lateral dynamics. In addition, robust controllers have been used, such as H_∞ control [5], and a feedback controller [6].

It is commonly known that sliding mode control (SMC) motion introduced by Utkin [7], is usually robust with respect to disturbances and uncertainty. Therefore, the SMC approach may effectively suppress the lumped disturbances by adding a switching control law to the control input. The SMC approach ensures asymptotic convergence of state variables. Some works have been concerned with additional requirements as finite-time stability. Bhat and Bernstein first established finite-time stability in [8] before applying it to finite-time stabilization, as seen in [9] among other works. Depending on the initial conditions, it makes sure that dynamical systems attain their equilibrium in a finite amount of time, known as settling time. Polyakov established the fixed-time stability in [10]. Fixed-time stability guarantees that the settling time is independent of the beginning circumstances in addition to finite-time stability. For engineering applications, fixed-time stabilization offers a predetermined convergence period toward the equilibrium.

SMC has been used for autonomous vehicles in several works [11]- [17]. For example, the tracking performance of autonomous vehicle systems has been enhanced by the structural innovation and widespread application of SMC [12], [13]. The finite-time control using a nonsingular terminal sliding mode controller was studied in [11] for the lateral control of autonomous vehicles.

Based on the above works and inspired by finite-time (FnT) and fixed-time (FxT) controllers, a fixed-time controller combined with a nonsingular terminal sliding mode variable is proposed for the first time in this paper for the lateral dynamics of autonomous vehicles. Using a nonsingular terminal sliding mode variable, the lateral deviation and orientation error converging to zero in a finite time. The upper bound of disturbances affecting vehicle dynamics is coped with the fixed-time switching law. The latter used the sliding variable exponent coefficients. The proposed controller ensures for lateral dynamics time-independent settling time, nonsingularity, is easy to implement, and robust against disturbances. The main contributions of this work are:

- The finite-time convergence of the lateral and orientation errors, is ensured based on a nonsingular terminal sliding variable.
- A switching control that has a sliding variable exponent coefficient is synthesised to ensure the fixed-time stability of the closed-loop lateral system.
- Several nonlinear simulations under complex situations are given and a comparative study is presented with the proposed control method.

The outline of the paper is as follows. The vehicle modeling and problem formulation are given in Section II. Preliminary theorems on finite/fixed time are presented in Section IV. Section II. Section IV is dedicated to designing a nonsingular terminal sliding-mode control of autonomous vehicles with global fixed-time stability guarantees. The nonlinear simulations with some scenarios are given in Section V. The last Section V concludes the paper.

II. Vehicle modeling and problem formulation

Assumption 1: The longitudinal speed v_x is assumed be constant and strictly positive.

Under the assumptions presented in [6], [22], Assumption 1 and using the well-known Newton's Second Law for motion along the lateral axis, the equations for the yaw dynamics are produced by the moment balance about the vertical axis

[1]Univ. Grenoble Alpes, CNRS, Grenoble INP, GIPSA-lab, 38000 Grenoble, France moussa.labbadi,olivier.sename@grenoble-inp.fr

Fig. 1. Autonomous Robot ciTHy M (https://www.twinswheel.fr/).

TABLE I

SYSTEM ABBREVIATIONS, NOTATION, AND PARAMETERS.

v_y, v_x	lateral and longitudinal velocities
δ, ψ	vehicle steering and yaw angles
y_L, ψ_L	lateral and heading error
ρ, μ	curvature and road friction
m, I_z	mass and z inertia $(160kg, 40kg.m^2)$
C_f, C_r	tires stiffness $(6e3, 5e5)N/rad$
l_f, l_r	wheelbase $(0.8, 0.7)m$
l_w, l_s	preview distance $(0.4, 0.5)m$

[6], [22].

$$\begin{aligned}\dot{v}_y =& -v_x r + \frac{1}{m}(F_{yf} + F_{yr} + F_{wy})\\ \dot{r} =& \frac{1}{I_z}(l_f F_{yf} - l_r F_{yr} + l_w F_{wy})\end{aligned} \tag{1}$$

where F_{yf} and F_{yr} are respectively the front and rear wheels' lateral tyre forces. r is the yaw rate, v_x represents the longitudinal speed. m is the total mass. I_z stands for the vehicle's moment of inertia about the yaw axis, and l_f and l_r stand for the front and rear tires' respective distances from the mass center of the vehicle.

The aerodynamic and tire/road interaction forces are the primary external forces acting on the vehicle while it is moving. While the tire's lateral slip forces F_{yi} are approximated by linear stiffness with respect to the tire slip angles, the side wind force F_{wy} is considered to be an external perturbation in this situation. Consequently, the state representation of the dynamic of the lateral vehicle is provided by

$$\begin{bmatrix}\dot{v}_y\\ \dot{r}\end{bmatrix} = \begin{bmatrix}\overbrace{-2\mu\frac{C_f + C_r}{v_x m}}^{f_1} & \overbrace{2\mu\frac{-C_f l_f + l_r C_r}{v_x m} - v_x}^{f_2}\\ \underbrace{2\mu\frac{-l_f C_f + l_r C_r}{v_x I_z}}_{f_3} & \underbrace{-2\mu\frac{C_f l_f^2 + l_r^2 C_r}{v_x I_z}}_{f_4}\end{bmatrix}\begin{bmatrix}v_y\\ r\end{bmatrix} + \begin{bmatrix}\overbrace{2\mu\frac{C_f}{m}}^{g_1}\\ \underbrace{\frac{\mu l f C_f}{I_z}}_{g_2}\end{bmatrix}\delta + \begin{bmatrix}1\\ l_w\end{bmatrix}F_{wy} \tag{2}$$

All parameters presented in (2) are defined in Table I. These parameters correspond to an autonomous robot. The robot is from the SOBEN company of a small four wheels "ciTHy M" range (see Fig. 1). This autonomous robot is used for meal distribution and home delivery.

The vehicle positioning factors with regard to the traffic lanes must be understood in order to create a controller for a driving aid system. In order to minimize position and orientation errors in relation to the planned trajectory, it is required to maintain careful tracking of the reference trajectories provided by a planning module. This implies that the heading error ψ_L and the lateral error y_L should converge in finite-time to zero and that the vehicle axis should always be parallel to the planned trajectory tangent axis and the vehicle lateral deviation always be close to the nearest trajectory point. The dynamics of both variables used in this paper are [21]

$$\begin{aligned}\dot{\psi}_L =& r - \rho v_x\\ \dot{y}_L =& v_y + \psi_L v_x + r l_s\end{aligned} \tag{3}$$

where ρ denotes the curvature of the reference trajectory (lane curvature). Note that the graphical definitions of the variables are illustrated in Fig. 2. The following formulation

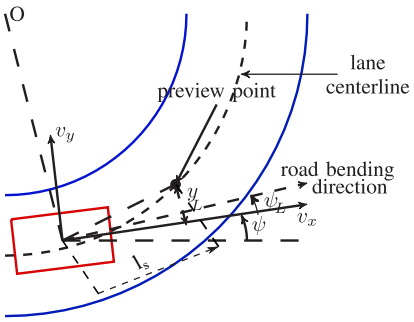

Fig. 2. Graphical definitions of variables y_L and ψ_L in lane keeping cases;

represents the control problem for lateral motion to find a robust controller such that the closed-loop system has the following characteristics given the system (2)-(3) and the time history of the feasible road curvature $\rho(t)$.

- P_1) The control effort $\delta(t)$ is bounded and satisfying $\delta(t) \leq \delta_{max}$ and $|\dot{\delta}(t)| \leq v_{max}$.
- P_2) the tracking errors converge to zero in finite-time and the state variables $v_y(t)$ and $r(t)$ converge to their references $v_{yr}(t)$ and $r_r(t)$ in short finite-time.
- P_3) the closed-loop system (2), (3) with the designed controller is fixed-time stable.

III. PRELIMINARIES ON FINITE/FIXED TIME STABILITY

Some definitions of finite/fixed-time stability are recalled. Consider the following system.

$$\dot{z}(t) = \mathcal{F}(z(t)), \quad z(t) \in \mathbb{R}^n \tag{4a}$$

$$z(0) = z_0, \quad \mathcal{F}(0)) = 0. \tag{4b}$$

In the system (4a), $\mathcal{F}(z(t))$ is a continuous function.

Definition 1: Refer to [8], [9] and consider the system (4a) and its candidate Lyapunov function (CLF) $V(z(t))$ with $V(z(0)) = V(z_0)$ denotes the initial condition of CLF then the system (4a) is globally FnT stable if it is CLF stable for

all $z_0 \in \mathbb{R}^n$ there exists the settling time satisfying $\mathcal{T}(z_0) \geq 0$. $\mathcal{T}(z_0)$ depends on initial conditions

Definition 2: [10] System (4a) is globally FxT stable if:

- (4a) is global FnT stable.
- $\mathcal{T}(z_0) \leq \mathcal{T}$, which $\mathcal{T}$ is a constant for a given z_0.

Lemma 1: Consider the CLF as:

$$\dot{V}(z) \leq -\beta_1 V(z)^{\alpha_1} - \beta_2 V(z)^{\alpha_2} \tag{5}$$

with $\beta_1, \beta_2 > 0$ and $0 < \alpha_1 < 1 < \alpha_2$, then (4a) is global FxT stable and the settling time satisfies

$$\mathcal{T}(z_0) \leq \frac{1}{\beta_1(1-\alpha_1)} + \frac{1}{\beta_2(1-\alpha_2)} \tag{6}$$

IV. Fixed-time lateral control with nonsingular terminal sliding mode for autonomous vehicles

In order to design the lateral controller, the total system is viewed as an interconnected system. There is little doubt that the "Lateral Dynamics of the Vehicle" is the primary subsystem of the open-loop system, which also includes the "Lane Keeping Dynamics" and the "Steering System". The main results of this paper are addressed in this section. Consider the error surface to reduce lane tracking position and orientation errors as:

$$e = c_1 l_p \psi_L + c_2 y_L, \tag{7}$$

To balance the impact of the lateral deviation error and the heading error on the convergence of the sliding surface, $c_i > 0, i = 1, 2$ are design parameters that need to be adjusted. These sliding surface gains have been suggested in SMC literature [7] for the design of the surface gains and are simple to assure sliding surface convergence. Given that the system's relative degree to the error under consideration is 2, a linear sliding surface can be defined as:

$$s = \dot{e} + \beta_1 e, \tag{8}$$

By setting the time derivative of s as

$$\dot{s} = \ddot{e} + \beta_1 \dot{e}, \tag{9}$$

and another hand, the dynamic of s is chosen as,

$$\dot{s} = -\frac{K}{\{(c_1 l_p + c_2 l_s) g_2 + c_2 g_1\}} sign(s), \tag{10}$$

The double derivative of (7) is,

$$\begin{aligned}\ddot{e} =& \{(c_1 l_p + c_2 l_s) g_2 + c_2 g_1\}\delta + (c_1 l_p + c_2 l_s)(f_3 v_y + f_4 r) \\ &+ c_2(f_1 v_y + f_2 r) - c_1 l_p \dot{\rho} v_x + c_2 \dot{\psi}_L v_x,\end{aligned} \tag{11}$$

From (9), (10), and (11), the control law can be given:

$$\begin{aligned}\delta =& -\frac{1}{\{(c_1 l_p + c_2 l_s) g_2 + c_2 g_1\}}[(c_1 l_p + c_2 l_s)(f_3 v_y + f_4 r) \\ &+ c_2(f_1 v_y + f_2 r) - c_1 l_p \dot{\rho} v_x + c_2 \dot{\psi}_L v_x + \beta_1 \dot{e} + K sign(s)]\end{aligned} \tag{12}$$

Proposition 1: If $K > d \geq |c_2 F_{wy} + l_w F_{wy}(c_1 l_p + c_2 l_s)|$, the closed-loop system (1), (3), (7), (8) and (12) is globally asymptotically stable and the tracking errors (y_L, ψ_L) are converging to zero.

Proof: Consider the Lyapunov function $V = \frac{1}{2}s^2$. We can prove that:

$$\begin{aligned}\dot{V} =& s(-K sign(s) + c_2 F_{wy} + l_w F_{wy}(c_1 l_p + c_2 l_s)) \\ \leq& -(K - d)|s| \\ \leq& 0.\end{aligned} \tag{13}$$

■

Note that $\dot{e} = -\beta_1 e$ when the sliding surface is reached, ensuring the closed loop system's (1), (8), (7), and (12) asymptotic stability in the direction of the origin. In the next part, a non-singular terminal sliding mode manifold is presented for the system to ensure the finite-time convergence of both tracking errors.

Lemma 2 ([18]): Consider the sliding variable

$$s = \ddot{e} + \kappa_2 |\dot{e}|^{\mu_2} sign(\dot{e}) + \kappa_1 |e|^{\mu_1} sign(e), \tag{14}$$

where μ_j and κ_j $(j = 1, 2)$ are positive constants such that the polynomial $p^2 + \kappa_2 p + \kappa_1$ is Hurwitz and

$$\begin{cases} \mu_1 & = \mu_0, \\ \mu_2 & = \frac{\mu_1 \mu_2}{2\mu_2 - \mu_1}. \end{cases} \tag{15}$$

Once the sliding mode is established (i.e., $s = 0$), the system state converges to zero in FnT.

Assumption 2: Define the disturbances

$$d(t) = c_2 F_{wy} + l_w F_{wy}(c_1 l_p + c_2 l_s) \tag{16}$$

and assuming its derivative as $\dot{d}(t) \leq d_1$ with $d_1 > 0$.
The equivalent control law can be obtained by setting $s = 0$ and $d(t) = 0$. Thus, one has

$$\begin{aligned}\delta_{eq} =& -\frac{1}{\{(c_1 l_p + c_2 l_s) g_2 + c_2 g_1\}}[c_2(f_1 v_y + f_2 r) \\ &+ (c_1 l_p + c_2 l_s)(f_3 v_y + f_4 r) - c_1 l_p \dot{\rho} v_x \\ &+ c_2 \dot{\psi}_L v_x + \kappa_2 |\dot{e}|^{\mu_2} sign(\dot{e}) + \kappa_1 |e|^{\mu_1} sign(e)]\end{aligned} \tag{17}$$

Remark 1: In [19] when $s = 0$ in (14), it has been proved that the system state converges to zero in finite time. The same for the lateral control of (1), given the parameters μ_j and κ_j then both tracking errors (y_L, ψ_L) converge to zero in a finite-time referred to as T_1.

Employing the non-singular terminal sliding-dependent variable power coefficient in the reaching control law to address the disturbances problem and to ensure the fixed-time stability of the lateral system (2). Based on the work developed in [20], the fixed-time controller is given by:

$$\dot{\delta}_s = -\frac{1}{\{(c_1 l_p + c_2 l_s) g_2 + c_2 g_1\}}[h|s|^{\frac{\lambda s^2}{1+\eta s^2}} sign(s)] \tag{18}$$

with $\eta, \lambda \in \mathbb{R}^{*+}$ such as $a = \frac{\lambda}{1+\eta} > 1$, and $h > d_1 e^{\frac{-\lambda}{4\sqrt{\pi}}}$. Then, the steering controller is resumed as:

$$\begin{aligned}\delta =& \delta_{eq} + \delta_s \\ =& -\frac{1}{\{(c_1 l_p + c_2 l_s) g_2 + c_2 g_1\}}[c_2(f_1 v_y + f_2 r) \\ &+ (c_1 l_p + c_2 l_s)(f_3 v_y + f_4 r) - c_1 l_p \dot{\rho} v_x \\ &+ c_2 \dot{\psi}_L v_x + \kappa_2 |\dot{e}|^{\mu_2} sign(\dot{e}) + \kappa_1 |e|^{\mu_1} sign(e) \\ &h \int (|s|^{\frac{\lambda s^2}{1+\eta s^2}} sign(s)) d\tau]\end{aligned} \tag{19}$$

Theorem 1: Consider the vehicle lateral model in (1)-(3) where $d(t)$is defined as (16) and satisfies the Assumption 2, then the closed-loop lateral extended system (1), (3), (7), (8), (14), and (19) is globally finite-time stable and the settling time satisfies

$$T_g \leq T_1 + \frac{1}{2^{\alpha}(h-d_1)(\alpha-1)} + \frac{2^{\frac{1}{2}}}{(he^{\frac{-\lambda}{2e}} - d_1)} \tag{20}$$

However, the variables y_L and ψ_L converge to zero in an FnT T_g.

Proof: From the system (2) and (3), the nonsingular terminal sliding mode variable can be rewritten as:

$$\begin{aligned} s =& \{(c_1 l_p + c_2 l_s)g_2 + c_2 g_1\}\delta + (c_1 l_p + c_2 l_s)(f_3 v_y + f_4 r) \\ &+ c_2(f_1 v_y + f_2 r) - c_1 l_p \dot{\rho} v_x + c_2 \dot{\psi}_L v_x \\ &+ \kappa_2 |\dot{e}|^{\mu_2} sign(\dot{e}) + \kappa_1 |e|^{\mu_1} sign(e) \end{aligned} \tag{21}$$

Using (17) into (21) results in:

$$s = -h \int (|s|^{\frac{\lambda s^2}{1+\eta s^2}} sign(s)) d\tau + d(t) \tag{22}$$

Consider now the subsequent quadratic Lyapunov function and its time derivative as:

$$V = 0.5 s^2, \quad \dot{V} = s\dot{s}. \tag{23}$$

with $\dot{s} = -h|s|^{\frac{\lambda s^2}{1+\eta s^2}} sign(s) + \dot{d}(t)$. One obtains

$$\begin{aligned} \dot{V} =& -sh|s|^{\frac{\lambda s^2}{1+\eta s^2}} sign(s) + s\dot{d}(t) \\ \leq& -h|s|^{\frac{\lambda s^2}{1+\eta s^2}+1} + |s| d_1 \end{aligned} \tag{24}$$

Remark 2: The fixed-time controller proposed by Moulay et al. [20] can be presented as

$$\dot{V} = -2sh|s|^{\frac{\lambda s^2}{1+\eta s^2}} sign(s) + 2sd(t). \tag{25}$$

Therefore, the proposed fixed-time stability in [20] depends on the disturbance $d(t)$. However, the stability analysis reported in (24) depends on the derivative of disturbances $\dot{d}(t)$.

Similar to the work developed in [20], we have two cases:

- When $V(s) \geq 1$, then one has $\frac{\lambda s^2}{1+\eta s^2}+1 \leq \frac{\lambda}{1+\eta}+1 > 2$. Define $\alpha = \frac{\lambda}{1+\eta} + 1$. One get

$$\begin{aligned} \dot{V} \leq& -(h-d_1)|s|^{\frac{\lambda}{1+\eta}+1} \\ \leq& -(h-d_1)2^{\frac{\alpha+1}{2}} V^{\frac{\alpha+1}{2}} \end{aligned} \tag{26}$$

  As $h - d_1 > 0$ and $\frac{\alpha+1}{2} > 1$. Based on Lemma 2 and [20], the solution of (26) reaches in fixed-time $T_2 = \frac{1}{2^{\alpha}(h-d_1)(\alpha-1)}$.
- Consider the second case when $V(s) \leq 1$, from the result of theorem 1 in [20], we have

$$\dot{V} \leq -(he^{\frac{-\lambda}{2e}} - d_1)2^{\frac{1}{2}} V^{\frac{1}{2}}. \tag{27}$$

  As $h - d_1 > 0$ and based on Lemma 2, the solution of (27) reaches in fixed-time $T_3 \leq \frac{2^{\frac{1}{2}}}{(he^{\frac{-\lambda}{2e}} - d_1)}$.

Finally, system (2) reaches the origin in a fixed time $T_s \leq T_2 + T_3$ and the global system including the tracking errors (3) and variable sliding (14) reaches in finite-time $T_g \leq T_1 + T_2 + T_3$. ■

V. Simulation Results and Analysis

A nonlinear vehicle dynamics model is used in the simulation to evaluate the performances of the previously presented methodologies. This model enables the simulation of 7DOF: yaw angle, longitudinal and lateral displacements, and the four-wheel angular velocities to see then with the tire longitudinal slip. To show the effectiveness of the developed FxTSMC with nonsingular terminal sliding manifold, two case studies are presented: uniform circular motion and a realities trajectory from real data. To demonstrate the interest of the proposed FxTSMC, the classical SMC and back-stepping controllers are used for the comparison [23]. The resistive wind force is represented by the external disturbance in all of the aforementioned circumstances by the equation $F_{wy} = c_y v_x^2$. The control parameters are: $\mu_1 = \frac{9}{16}$, $\mu_2 = \frac{9}{23}$, $\kappa_1 = 192$, $\kappa_2 = 72$, $h = 2$, and $\eta = 0.1$. It should be noted that in both scenarios, the car is driven at a constant forward speed of $v_x = 8m/s$. Additionally, Table I provides the parameter values for the 7DOF vehicle in each simulation.

A. Case 1: Uniform Circular Motion

The curvature of trajectory in this case is assumed constant as $\rho(t) = 0.02$. In other words, the vehicle following a consistent circular motion. Be aware that in the case study, we make the assumption that the reference trajectory abruptly transforms at $t = 0$ into a circle with a radius of $50m$. The performance of the FxTSMC, backstepping, and SMC techniques as represented in Fig. 3. It is clear that the proposed FxTSMC (19) is capable of controlling the system because all four crucial variables related to the vehicle's lateral dynamics converge to reference values. Backstepping

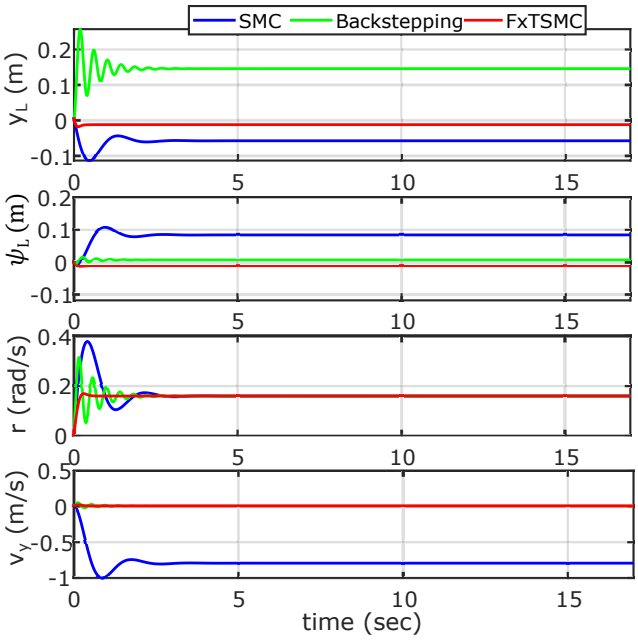

Fig. 3. Case 1: Illustration of the lateral deviation y_L , heading error ψ_L, yaw rate r and lateral speed v_y: (solid blue) SMC, (solid green) backstepping, and the proposed controller (solid red).

and SMC techniques are not capable enough to accurately track the desired values of the system in this situation.

Additionally, while the path's curvature is consistent, the vehicle equipped with either controller can follow the reference path precisely. However, it is evident by comparing the simulation results for the variables ψ_L, y_L, r, and v_y that the closed-loop system's response time with the provided FxTSMC controller is far faster than that of the other controllers. In comparison to the closed-loop system with backstepping and SMC approaches, the lateral deviation is almost negligible with the FxTSMC within 0.5 seconds. Additionally, by using the FxTSMC, the maximum lateral deviation is lowered from $0.2m$ (backstepping) and $-0.1m$ (SMC) to $0.02m$. The steering input control provided by the

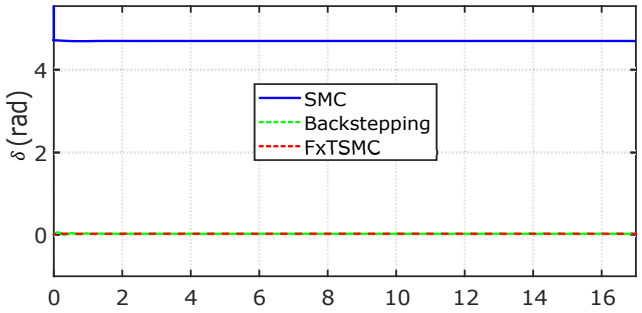

Fig. 4. Case 1: Illustration of the steering control: (solid blue) SMC, (dashed green) backstepping, and the proposed controller (dashed red).

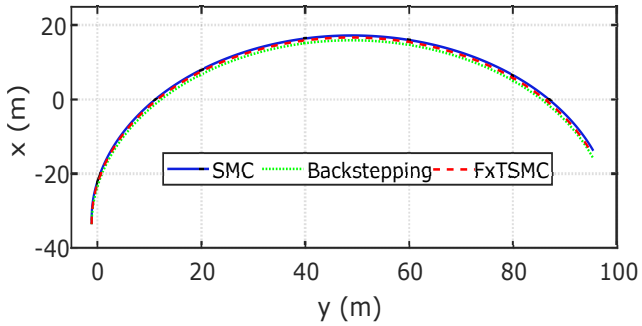

Fig. 5. Case 1: Illustration of the trajectory: (solid blue) SMC, (dashed green) backstepping, and the proposed controller (dashed red)

SMC have a chattering problem and have high amplitudes as presented in Fig. 4. The xy trajectory is plotted in Fig. 5, which the three controllers track the desired trajectory.

B. Case 2: Curvature for a real trajectory

In this case, the reference of the curvature is presented in Fig. 6. Figure 7 is depicted the four variables y_L, ψ_L, r, and v_y. The results of this scenario confirm the above three cases, in which the backstepping approach provided a high deviation in the error lateral motion and the other three variables are similar with more some performances on the FxTSMC. It is clear that the proposed FxTSMC provided a good settling time for a closed-loop system for all scenarios than the backstepping and SMC approaches. For example, the settling-time in case 1 satisfying $T_g < 0.4$ seconds, which

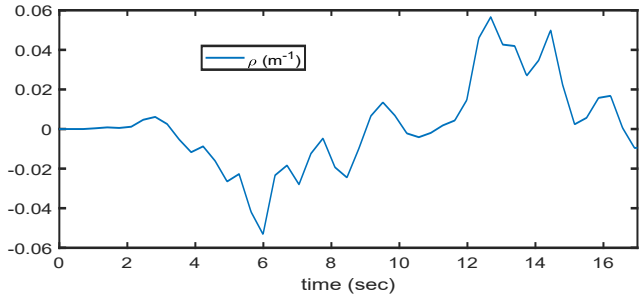

Fig. 6. Case 2: Road map curvature.

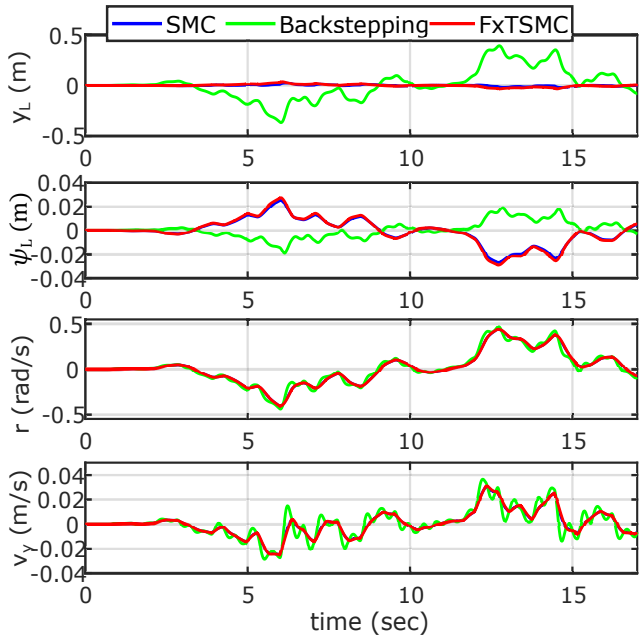

Fig. 7. Case 2 : Illustration of the lateral deviation y_L , heading error ψ_L, yaw rate r and lateral speed v_y: (solid blue) SMC, (solid green) backstepping, and the proposed controller (solid red).

demonstrates the results of Theorem 1. In other words, the lateral error converges to the desired value in a finite-time and has a faster response compared to other controllers.

Figures 9 and 8 show respectively the input control and the xy trajectory of three controllers in the case 2.

We note that the closed-loop system with the fixed-time settles in less than $0.3s$ regardless of the reference by comparing the settling times for the three scenarios. In other words, regardless of the variance in the variable ρ, the lateral deviation and heading error tend to zero, which coincide requires the vehicle to operate and these results are similar to some LPV approaches recently published as [3], [21].

VI. Conclusions

A solution to the fixed-time stability of the closed-loop lateral system of an autonomous vehicle has been proposed. The lateral controller solution is based on both a fixed-time switching approach that provided fixed-time stability against disturbances/external factors and a nonsingular terminal sliding mode manifold that ensured the finite-time convergence of the lateral deviation and the orientation error.

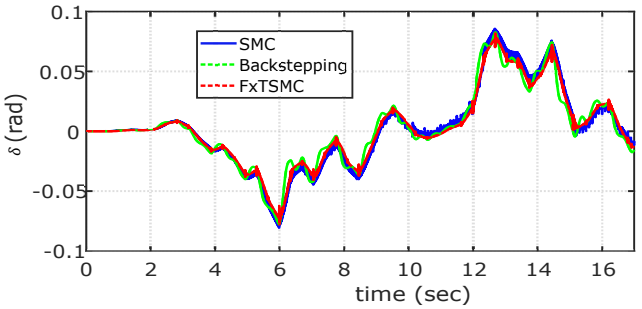

Fig. 8. Case 2: Illustration of the steering control: (solid blue) SMC, (dashed green) backstepping, and the proposed controller (dashed red).

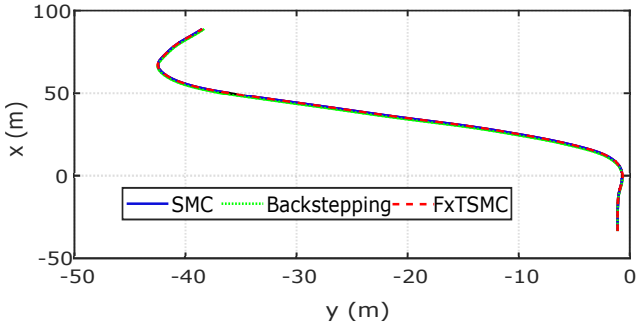

Fig. 9. Case 2: Illustration of the trajectory: (solid blue) SMC, (dashed green) backstepping, and the proposed controller (dashed red)

The proposed ultimate controller design of lateral dynamics takes into account the external disturbances. The fixed-time stability of the closed-loop lateral system has been proposed based on Lyapunov theory. The nonlinear simulation results with several changes in lane and trajectory tracking shows that the proposed FxTSMC approach is better compared to the classical SMC and backstepping technique.

ACKNOWLEDGMENT

The authors gratefully acknowledges the financial support from the ANR (French National Research Agency) through the project by FRANCE RELANCE Grenoble INP- SOBEN.

REFERENCES

[1] B. Paden, M. Čáp, S. Z. Yong, D. Yershov, and E. Frazzoli, "A survey of motion planning and control techniques for self-driving urban vehicles," IEEE Trans. Intell. Veh., vol. 1, no. 1, pp. 3355, 2016.

[2] M. Rokonuzzaman, N. Mohajer, S. Nahavandi, and S. Mohamed, "Review and performance evaluation of path tracking controllers of autonomous vehicles," IET Intell. Transp. Syst., vol. 15, no. 5, pp. 646670, 2021.

[3] H. Atoui, O. Sename, V. Milanes, and J. J. Martinez, "LPV-Based Autonomous Vehicle Lateral Controllers: A Comparative Analysis," IEEE Trans. Intell. Transp. Syst., vol. 23, no. 8, pp. 13570-13581, 2022.

[4] J. Yang and N. Zheng, "An expert fuzzy controller for vehicle lateral control," in Proc. IEEE Annu. Conf. Ind. Electron., 2007, pp. 880-885.

[5] X. Huang, H. Zhang, G. Zhang, and J. Wang, "Robust weighted gain-Scheduling H_∞ vehicle lateral motion control with considerations of steering system backlash-type hysteresis," IEEE Trans. Control Syst. Technol., vol. 22, no. 5, pp. 1740-1753, Sep. 2014.

[6] J. Jiang and A. Astolfi, "Lateral Control of an Autonomous Vehicle," IEEE Trans. Intell. Veh., vol. 3, no. 2, pp. 228-237, 2018.

[7] V. Utkin, "Variable structure systems with sliding modes," IEEE Trans. Autom. Control, vol. AC-22, no. 2, pp. 212-222, Apr. 1977.

[8] S. P. Bhat and D. S. Bernstein, "Finite-time stability of continuous au- tonomous systems," SIAM J. Control Optim., vol. 38, no. 3, pp. 751-766, 2000.

[9] Y. Hong, "Finite-time stabilization and stabilizability of a class of control-lable systems," Syst. Control Lett., vol. 46, no. 4, pp. 231-236, 2002.

[10] A. Polyakov, "Nonlinear feedback design for fixed-time stabilization of linear control systems," IEEE Trans. Autom. Control, vol. 57, no. 8, pp. 2106-2110, Aug. 2012.

[11] Z. Sun, J. Zou, D. He, and W. Zhu, "Path-tracking control for autonomous vehicles using double-hidden-layer output feedback neural network fast nonsingular terminal sliding mode," Neural Comput. Appl., vol. 34, no. 7, pp. 51355150, 2022.

[12] L. El Hajjami, E. M. Mellouli, and M. Berrada, "Neural Network Based Sliding Mode Lateral Control For Autonomous Vehicle," 2020 1st Int. Conf. Innov. Res. Appl. Sci. Eng. Technol. IRASET 2020, 2020.

[13] R. Talj, G. Tagne, and A. Charara, "Immersion and invariance control for lateral dynamics of autonomous vehicles, with experimental validation," 2013 Eur. Control Conf. ECC 2013, no. Iv, pp. 968973, 2013.

[14] S. H. Lee and C. C. Chung, "Predictive control with sliding mode for autonomous driving vehicle lateral maneuvering," Proc. Am. Control Conf., pp. 29983003, 2017.

[15] R. Wang, G. Yin, J. Zhuang, N. Zhang, and J. Chen, "The Path Tracking of Four-Wheel Steering Autonomous Vehicles via Sliding Mode Control," 2016 IEEE Veh. Power Propuls. Conf. VPPC 2016 - Proc., pp. 16, 2016.

[16] T. Ma, W. Wang, C. Yang, Y. Zhang, and Y. Li, "A Path Following Scheme using Sliding Mode Prediction Control for Autonomous Vehicle with Uncertainty Estimation," Proc. 34th Chinese Control Decis. Conf. CCDC 2022, vol. 8, no. 3, pp. 2227, 2022.

[17] R. Wang, G. Yin, and X. Jin, "Robust adaptive sliding mode control for nonlinear four-wheel steering autonomous Vehicles path tracking systems," 2016 IEEE 8th Int. Power Electron. Motion Control Conf. IPEMC-ECCE Asia 2016, pp. 29993006, 2016.

[18] Y. Feng, F. Han, and X. Yu, "Chattering free full-order sliding-mode control", Automatica, vol. 50, no. 4, pp. 1310-1314, 2014.

[19] Y. Hong, Y. Xu, and J. Huang, "Finite-time control for robot manipulators," Syst. Control Lett., vol. 46, no. 4, pp. 243-253, 2002.

[20] E. Moulay, V. Lchapp, E. Bernuau, and F. Plestan, "Robust Fixed-Time Stability: Application to Sliding-Mode Control," vol. 67, no. 2, pp. 1061-1066, 2022.

[21] D. Kapsalis, O. Sename, V. Milanes, and J. J. Molina, "A reduced LPV polytopic look-ahead steering controller for autonomous vehicles," Control Eng. Pract., vol. 129, no. December 2021, p. 105360, 2022.

[22] R. Rajamani, Vehicle Dynamics and Control. New York, NY, USA: Springer, 2012.

[23] A. Norouzi, M. Masoumi, A. Barari, and S. Farrokhpour Sani, "Lateral control of an autonomous vehicle using integrated backstepping and sliding mode controller," Proc. Inst. Mech. Eng. Part K J. Multi-body Dyn., vol. 233, no. 1, pp. 141151, 2019.